

Supporting Information

V₂O₅/Conductive Polymer Nanocables with Build-in Local Electric Field Derived from Interface Oxygen Vacancies for High Energy Density Supercapacitors

Wenchao Bi^{a, b}, *Juanjuan Huang*^{b, c}, *Mingshan Wang*^{b, d}, *Evan P. Jahrman*^e, *Gerald T. Seidler*^e,

Jichao Wang^a, *Yingjie Wu*^f, *Guohua Gao*^{a*}, *Guangming Wu*^{a*}, *Guozhong Cao*^{b*}

^a Shanghai Key Laboratory of Special Artificial Microstructure Materials and Technology, School of Physics Science and Engineering, Tongji University, Shanghai 200092, China.

^b Department of Materials Science and Engineering, University of Washington, Seattle, WA 98195-2120, United States.

^c MOE Key Laboratory for Magnetism and Magnetic Materials, School of Physical Science and Technology, Lanzhou University, Lanzhou 730000, China.

^d The Center of New Energy Materials and Technology, School of Materials Science and Engineering, Southwest Petroleum University, Chengdu, Sichuan 610500, PR China

^e Department of Physics, University of Washington, Seattle, WA 98195-1560, United States.

^f Department of Material Science and Engineering, Monash University, Clayton, Victoria 3800, Australia

*Email: gao@tongji.edu.cn (G.G);

*Email: wugm@tongji.edu.cn (G.W);

*Email: gzcao@u.washington.edu (G.C)

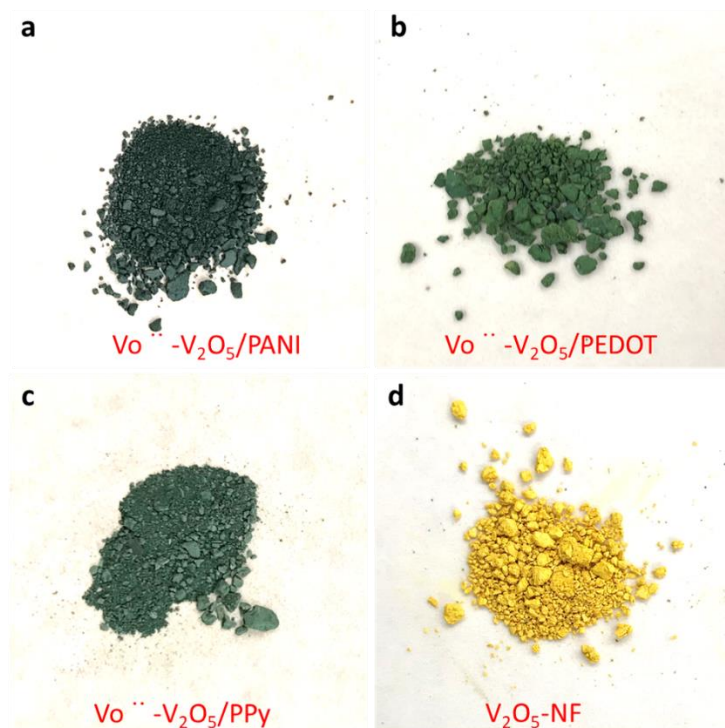


Figure S1. The digital images of $\text{Vo}^{2+}\text{-V}_2\text{O}_5/\text{CP}$ nanocables and $\text{V}_2\text{O}_5\text{-NF}$.

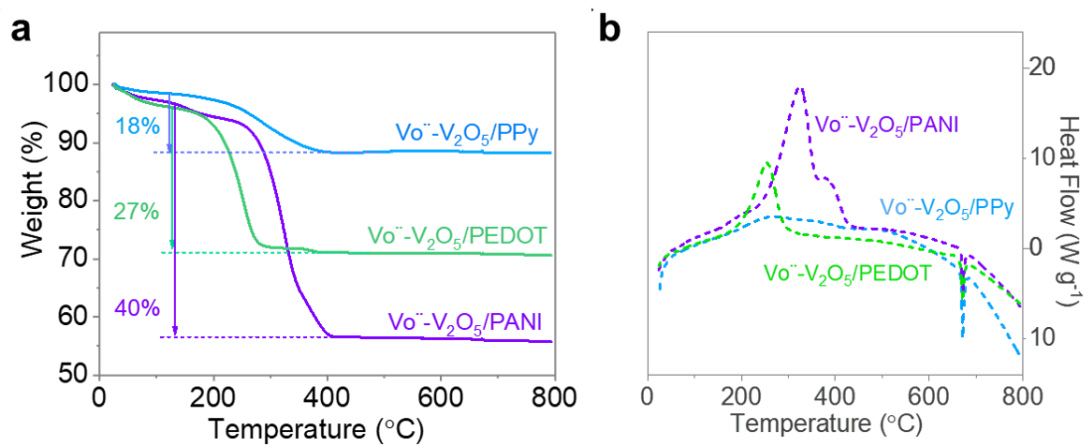


Figure S2. The TG-DSC curves of all $\text{Vo}^{2+}\text{-V}_2\text{O}_5/\text{CP}$ nanocables.

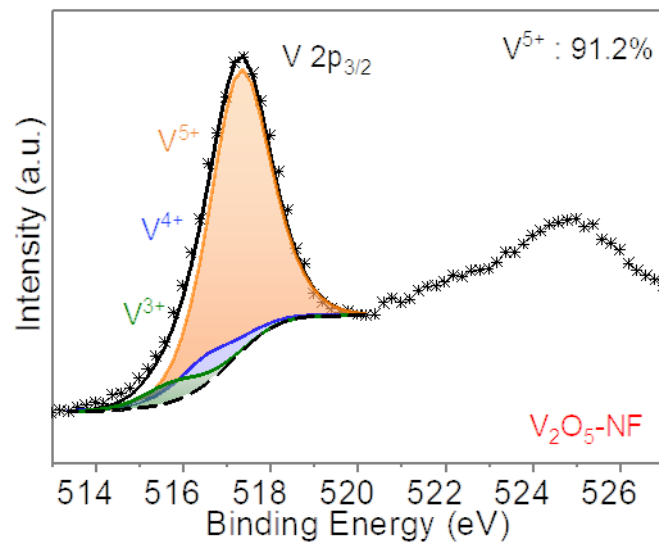


Figure S3. The XPS spectrum and corresponding decompositions of V 2p_{3/2} peak of V₂O₅-NF.

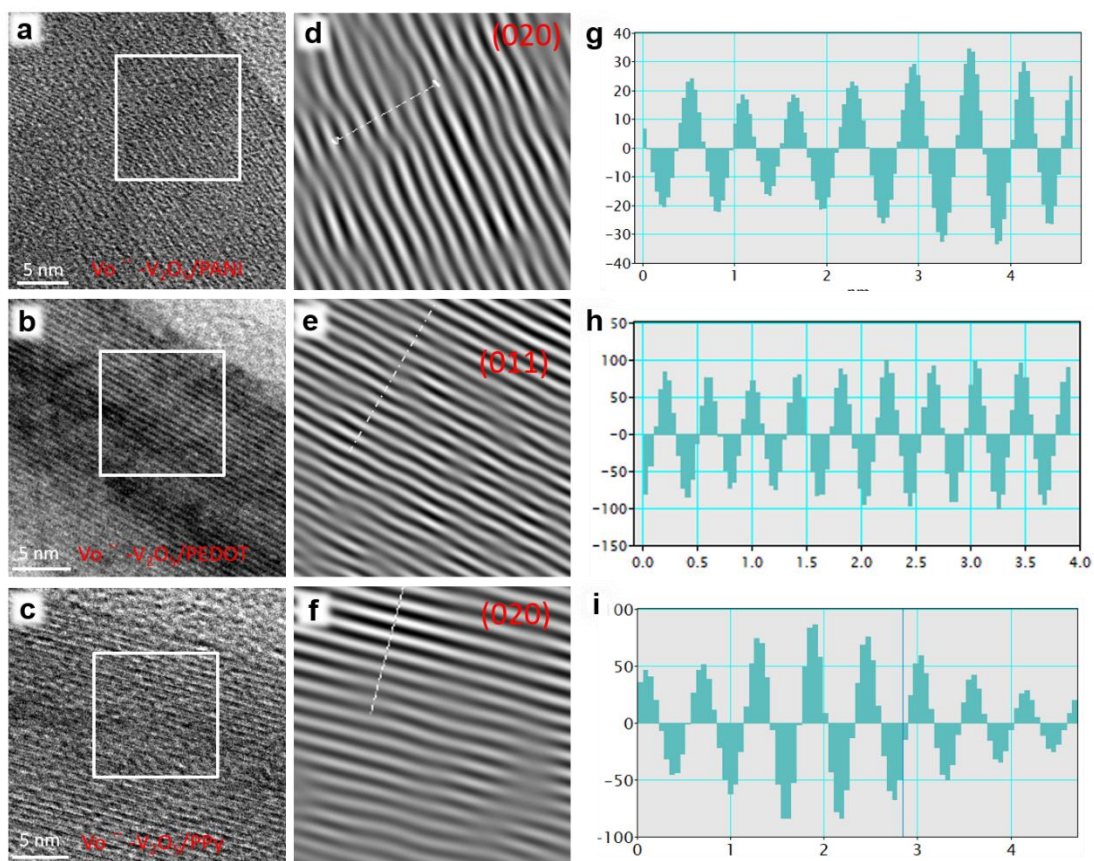


Figure S4. (a, b, c) HRTEM images of $\text{Vo}^{\bullet}\text{-V}_2\text{O}_5/\text{PANI}$, $\text{Vo}^{\bullet}\text{-V}_2\text{O}_5/\text{PEDOT}$ and $\text{Vo}^{\bullet}\text{-V}_2\text{O}_5/\text{PPy}$. (d, e, f) IFFT patterns of selected areas in HRTEM. The Vo^{\bullet} -caused dislocations can be easily observed. (e, f) Linear profiles obtained from the white lines in corresponding IFFT images, respectively. The interlayer spaces are expanded due to Vo^{\bullet} .

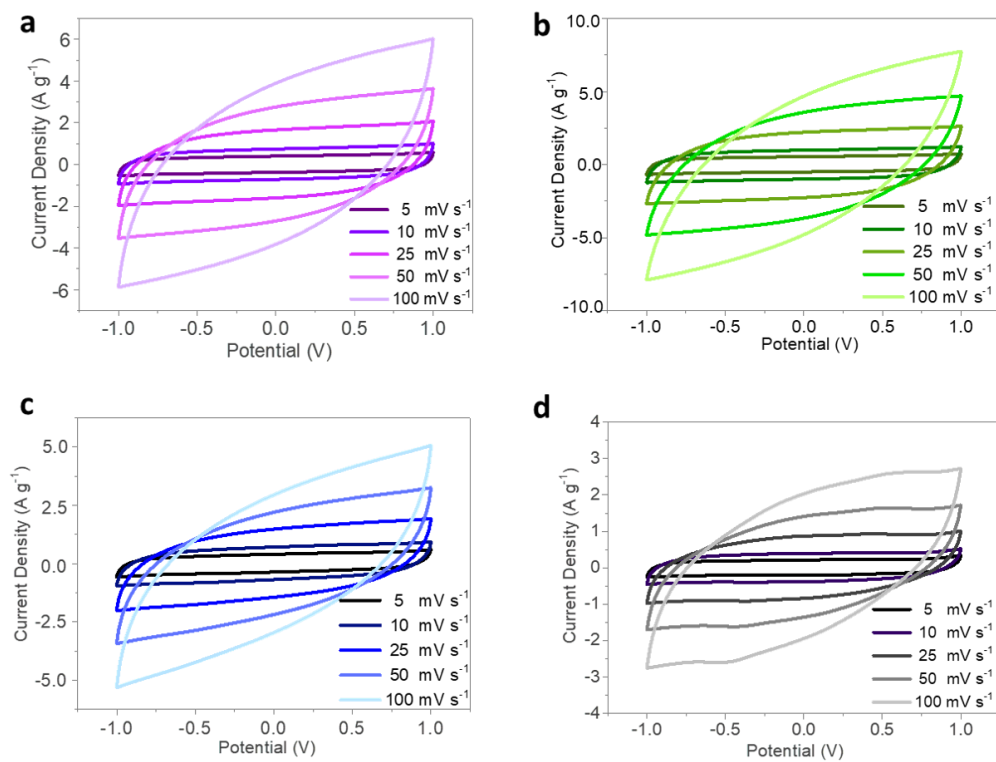


Figure S5. The CV curves of $\text{Vo}^{\bullet\bullet}\text{-V}_2\text{O}_5/\text{PANI}$, $\text{Vo}^{\bullet\bullet}\text{-V}_2\text{O}_5/\text{PEDOT}$, $\text{Vo}^{\bullet\bullet}\text{-V}_2\text{O}_5/\text{PPy}$ and $\text{V}_2\text{O}_5\text{-NF}$.

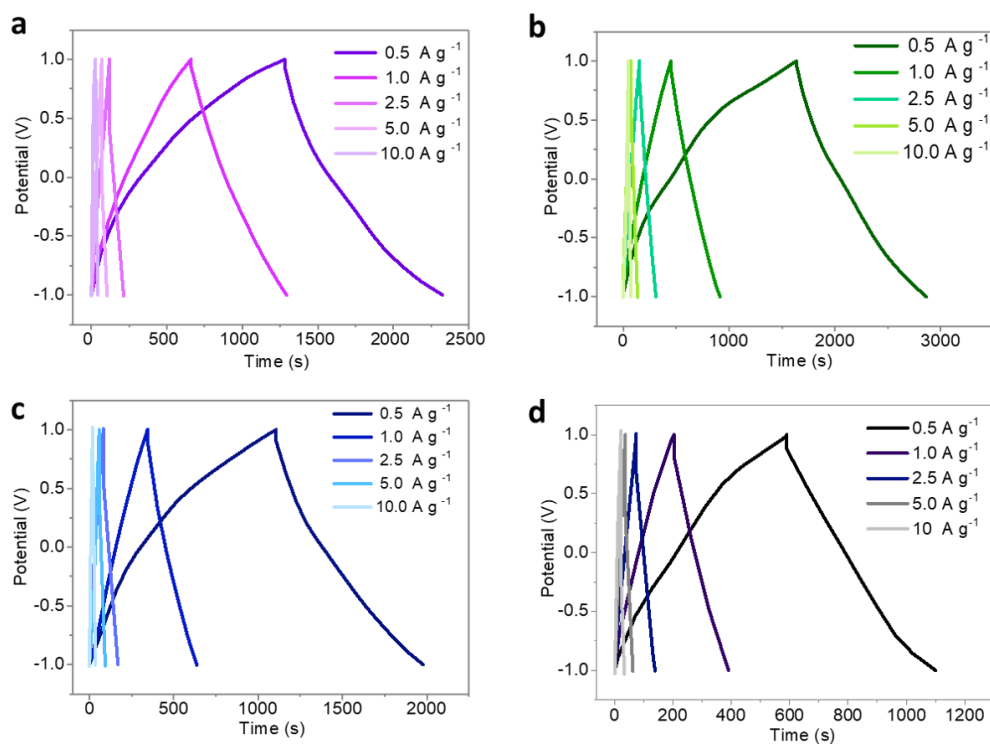


Figure S6. The GCD curves of (a) Vo²⁺-V₂O₅/PANI, (b) Vo²⁺-V₂O₅/PEDOT, (c) Vo²⁺-V₂O₅/PPy and (d) V₂O₅-NF.

	Vo ^{••} -V ₂ O ₅ /PEDOT	Vo ^{••} -V ₂ O ₅ /PANI	Vo ^{••} -V ₂ O ₅ /PPy	V ₂ O ₅ -NF
R _s (Ω)	0.5	0.6	0.5	0.7
R _{ct} (Ω)	2.3	3.0	5.9	8.4
σ _w	14.45	11.21	10.11	7.45
D _{Na⁺} (10 ⁻¹² cm ² /s)	9.54	5.17	4.12	2.51

Table S1. The R_s, R_{ct}, σ_w and D_{Na⁺} values of Vo^{••}-V₂O₅/PANI, Vo^{••}-V₂O₅/PEDOT, Vo^{••}-V₂O₅/PPy and V₂O₅-NF, which are obtained by ZsimpWin from EIS curves.

The Na⁺ ion diffusion coefficient of the electrode materials is calculated from the low frequency regions of corresponding EIS plots based on the following equation.

$$D_{Na^+} = \frac{R^2 T^2}{2 A^2 n^4 F^4 C^2 \sigma_w^2}$$

F is 96500 C·mol⁻¹) is the Faraday constant;

R (8.314 J·mol⁻¹·K⁻¹) is gas constant;

T(298 K) is the absolute temperature;

A (cm²) is the surface area of the electrode;

C (mol·cm⁻³) is concentration of Na⁺ ion in the electrolyte;

n is the number of electrons transferred per molecule;

σ_w is Warburg coefficient which is obtained by ZsimpWin software.

	V ^o -V ₂ O ₅ /PEDOT	V ^o -V ₂ O ₅ /PANI	V ^o -V ₂ O ₅ /PPy
σ (S/cm)	300-500	0.1-5	10-50
Coating thickness (nm)	5.0	6.7	3.5
R (Ω /nm)	17~28	1239~61941	247~1237

Table S2. The estimated R values of V^o-V₂O₅/CPs.

In $R = L/\sigma A$, A is cross sectional area of CP in a nanocable, σ is the Electrical conductivity and L is the length (nm). Here, the average diameter is estimated to be 35 nm according to the SEM and TEM images.

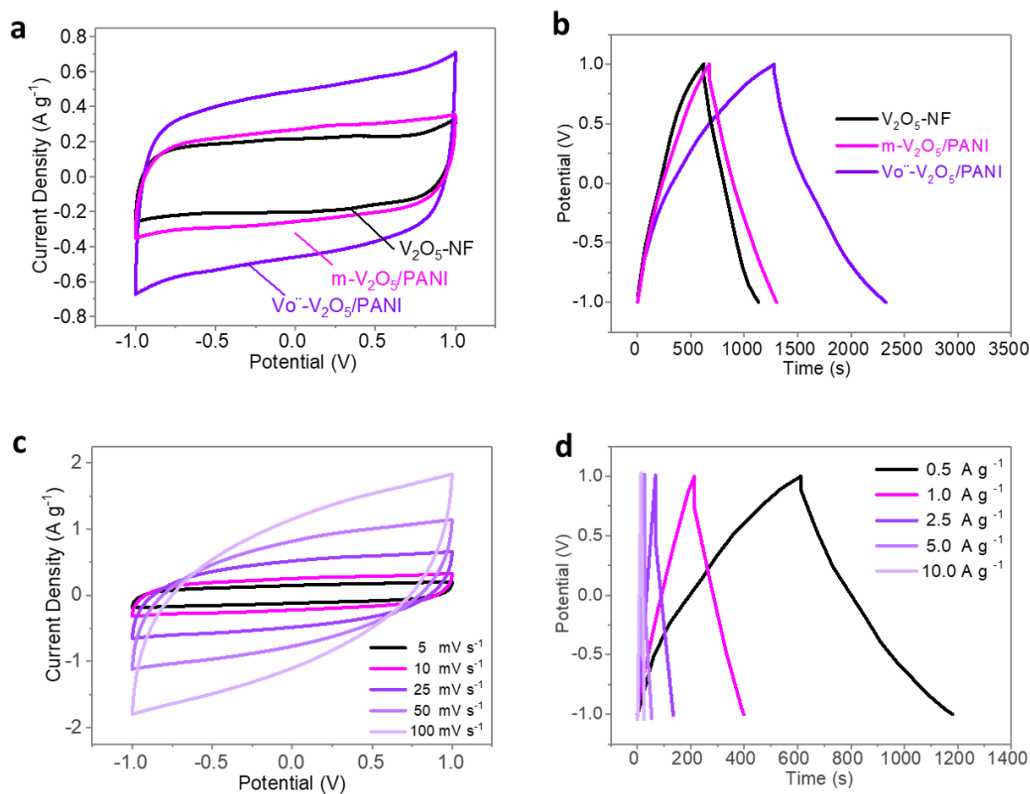


Figure S7. (a) The CV curves of $Vo''-V_2O_5/PANI$, $m-V_2O_5/PANI$ and V_2O_5 -NF at 5 mV s^{-1} . (a) The GCD curves of $Vo''-V_2O_5/PANI$, $m-V_2O_5/PANI$ and V_2O_5 -NF at 0.5 A g^{-1} . (c) The CV curves of $m-V_2O_5/PANI$ at different scan rates. (d) The GCD curves of $m-V_2O_5/PANI$ at different current densities.

Considering the CPs have similar function in our samples, and commercial PANI has the lowest price than PEDOT and PPy, which can be found on Sigma-Alorich company website, the synergistic effects of Vo'' and CPs are explored by taking $Vo''-V_2O_5/PANI$ for example. V_2O_5 -NF and commercial PANI are mechanically mixed with the mass ratio from the TG results, noted as $m-V_2O_5/PANI$. All the electrochemical measurements are conducted under the same conditions. As shown above, the $m-V_2O_5/PANI$ electrode shows a specific capacitance of 280 F g^{-1} at 0.5 A g^{-1} , which is smaller than that of $Vo''-V_2O_5/PANI$ (523 F g^{-1}), larger than that of V_2O_5 -NF (225 F g^{-1}). Thus, the excellent electrochemical performance of $Vo''-V_2O_5/CPs$ is attributed to the synergistic effects of Vo'' and CPs.

References